NASA TECHNICAL MEMORANDUM

NASA TM X-2081

NASA TM X-2081

EFFECT OF DYNAMIC VARIATIONS IN ENGINE-INLET PRESSURE ON THE COMPRESSOR SYSTEM OF A TWIN-SPOOL TURBOFAN ENGINE

by John E. McAulay

Lewis Research Center

Cleveland, Ohio 44135

NATIONAL AERONAUTICS AND SPACE ADMINISTRATION • WASHINGTON, D. C. • SEPTEMBER 1970

1. Report No. NASA TM X-2081	2. Government Accession No.	3. Recipient's Catalog No.
4. Title and Subtitle EFFECT OF DYNAMIC VARIATIONS IN ENGINE-INLET PRESSURE ON THE COMPRESSOR SYSTEM OF A TWIN-SPOOL TURBOFAN ENGINE		5. Report Date September 1970 6. Performing Organization Code
7. Author(s) John E. McAulay		8. Performing Organization Report No. E-5618
9. Performing Organization Name and Address Lewis Research Center National Aeronautics and Space Administration Cleveland, Ohio 44135		10. Work Unit No. 720-03 11. Contract or Grant No. 13. Type of Report and Period Covered Technical Memorandum
12. Sponsoring Agency Name and Address National Aeronautics and Space Administration Washington, D.C. 20546		14. Sponsoring Agency Code

15. Supplementary Notes

16. Abstract

The effects of spatially uniform and distorted dynamic engine-inlet pressure variations between 1 and 80 Hz on the compressor system of a twin-spool turbofan engine are presented. The inlet pressure variations were produced by rapid changes in secondary airflow injected as many small contrastream jets ahead of the engine. Compressor system stall was encountered with both spatially uniform and distorted dynamic variations in inlet pressure. The factors which induced compressor stall were found to be the magnitude of instantaneous distortion, rate and magnitude of change of inlet pressure, and dwell-time of the fan-compressor rotor blading in the low-pressure region of an engine-inlet distortion.

17. Key Words (Suggested by Author(s))	18. Distribution Statement
Turbofan engine Inlet pressure oscillations Compressor stall	Unclassified - unlimited

19. Security Classif. (of this report)	20. Security Classif. (of this page)	21. No. of Pages	22. Price*
Unclassified	Unclassified	33	$3.00

*For sale by the Clearinghouse for Federal Scientific and Technical Information Springfield, Virginia 22151

EFFECT OF DYNAMIC VARIATIONS IN ENGINE-INLET PRESSURE ON THE COMPRESSOR SYSTEM OF A TWIN-SPOOL TURBOFAN ENGINE

by John E. McAulay

Lewis Research Center

SUMMARY

An investigation was conducted to determine the effects of dynamic inlet pressure variations on the compressor system of a turbofan engine. These inlet pressure variations were produced by rapid changes in secondary airflow injected as many small contrastream jets ahead of the engine. The air jet system was mechanically capable of frequencies up to 200 hertz; however, due to the jet system and engine-inlet duct flow characteristics, measurable amplitudes in engine-inlet and fan-compressor system pressures were not achieved above 80 hertz.

The air jet system was used to produce cyclic variations in engine-inlet pressure with essentially zero instantaneous spatial distortion (uniform flow), 180° circumferential-extent distortion, and rotating distortion. In addition, single pressure pulses were introduced with uniform flow and 180° distortion.

Uniform cyclic inlet pressure variations resulted in transient changes in the fan-compressor stage group pressure ratios and in fan-compressor stall at high amplitudes (i.e., normalized inlet pressure amplitudes of 0.28 or greater). The changes in pressure ratio during the cyclic inlet pressure variation were largest for the fan tip, fan hub, and the high-compressor rear stage groups. Oscillating spatial distortions at the engine face resulted in compressor stall at substantially lower inlet pressure amplitudes than those required to produce stall with spatially uniform oscillating pressure variations. Stall was produced at lower values of circumferential distortions with the 180° pulsed distortions than with the 180° steady-state distortions. A comparison of the instantaneous distortion required to produce compressor stall for the oscillating 180° distortion, rotating distortion, 180° single pulse, and 180° steady-state distortion showed that stall tolerance is a function of the instantaneous distortion, the rate of change of the inlet pressure, and the dwell-time of the fan-compressor rotor blading in the low-pressure region of an engine-inlet distortion.

INTRODUCTION

One of the major problems encountered during the flight of supersonic aircraft is their inability to attain the desired flight attitudes, Mach numbers, and altitudes because of compressor stall. This restriction in aircraft operation is brought about by a combination of undesirable engine-inlet flow conditions produced by the engine-inlet system and the lack of adequate compressor stall margin at these inlet flow conditions. The interrelation between the engine inlet flow conditions and the compressor stall margin is not yet fully understood.

In the past the effect of steady-state distortion on engine performance and operation was determined by extensive testing using screens placed upstream of the engine inlet. References 1 and 2 are just a very small sampling of the reports describing this type of investigation. Reference 3 reports an early investigation (1958) of the effects of rapid inlet pressure oscillation on a turbojet engine. In recent years considerable interest has been invoked relative to the combined effects of steady-state distortion and inlet pressure dynamic variations. The work reported in references 4 and 5 are representative of investigations of this type.

An effort to continue this latter type of inquiry using a simpler and more basic approach has resulted in the experimental study reported herein. For this program a twin-spool turbofan engine was selected as being typical of those being planned for many advanced supersonic aircraft. High-response pressure instrumentation was used to provide an understanding of compressor system operation during dynamic inlet pressure variations.

To provide a controllable dynamic inlet flow environment, a new method of producing dynamic engine-inlet conditions was developed at Lewis Research Center. This method uses many small air jets upstream of the engine inlet and is reported in detail in references 6 and 7. Data were obtained while the turbofan engine was being subjected to spatially uniform and distorted (both cyclic and single pulse) and rotating inlet pressure variations. The cyclic variations were introduced at frequencies from 1 to 140 hertz. The results of these tests are presented as time histories of compressor pressures and stage group pressure ratios and compressor stall limits.

APPARATUS

Engine

The turbine engine used for this investigation was a twin-spool turbofan equipped with an afterburner. (See schematic of engine in fig. 1.) The engine consisted of a three-stage axial-flow fan mounted on the same shaft with a six-stage, axial-flow, low-

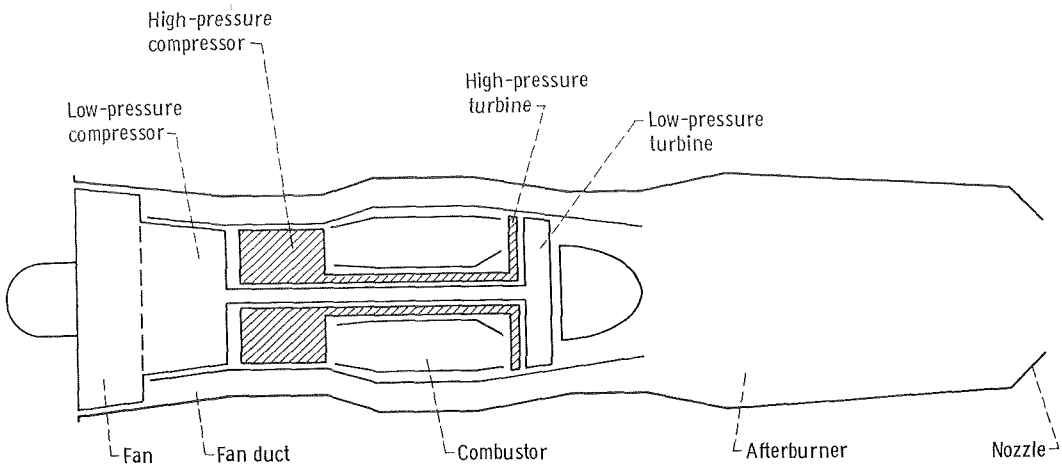

Figure 1. - Schematic diagram of twin-spool turbofan engine.

pressure compressor. This unit is driven by a three-stage, low-pressure turbine. The high-pressure spool is a seven-stage, axial-flow compressor driven by a single-stage, air-cooled turbine. The rated overall pressure ratio of the fan-compressor system is 17.0. The rated pressure ratio of the fan is 2.1, and it has a bypass ratio of 1.0. The compressor has two bleed systems located at about the middle of the low- and high-pressure compressors. Both of these bleed systems were closed during this investigation. The exhaust nozzle area was maintained at its rated value (3.65 ft^2 or 0.339 m^2).

Air Jet System

The air jet system, which was used to create the dynamic inlet pressure conditions at the engine face, was developed at Lewis Research Center (refs. 6 and 7). Its components are an inlet supply line, a positive shutoff gate valve, a flow supply butterfly valve, a torus or manifold and its associated piping, six servo-operated air jet valves of special design, and 54 lines (9 from each valve) supplying high-pressure air (secondary flow) to 54 jet nozzles located in the engine-inlet duct. A schematic sketch and photographs of this system are shown in figure 2. The jet nozzles, which had a throat diameter of 0.75 inch (1.91 cm), directed the secondary air counter to the primary flow which entered the engine after passing through the bellmouth.

The air jet system is supplied with 150 psia (103.5 N/cm^2 abs) air at temperatures between 60° and 90° F (16° and 32° C). The jet arrangement which is shown in figure 2(b) provides a uniformly distributed secondary flow which repeats every 60° of circumferential extent. The high-response servo-operated air jet valves, which are used

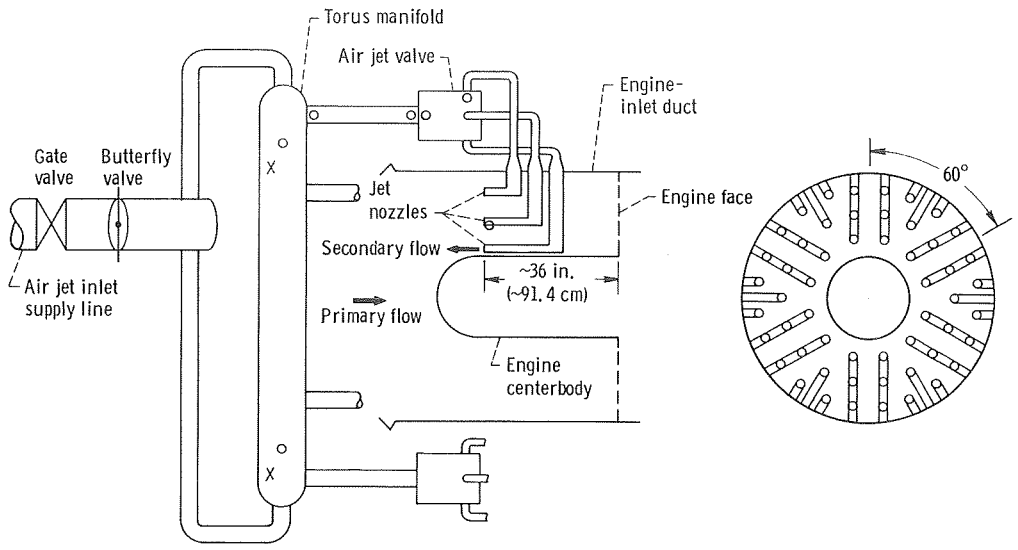

(a) Overall schematic.

(b) Frontal schematic of jets in engine-inlet duct.

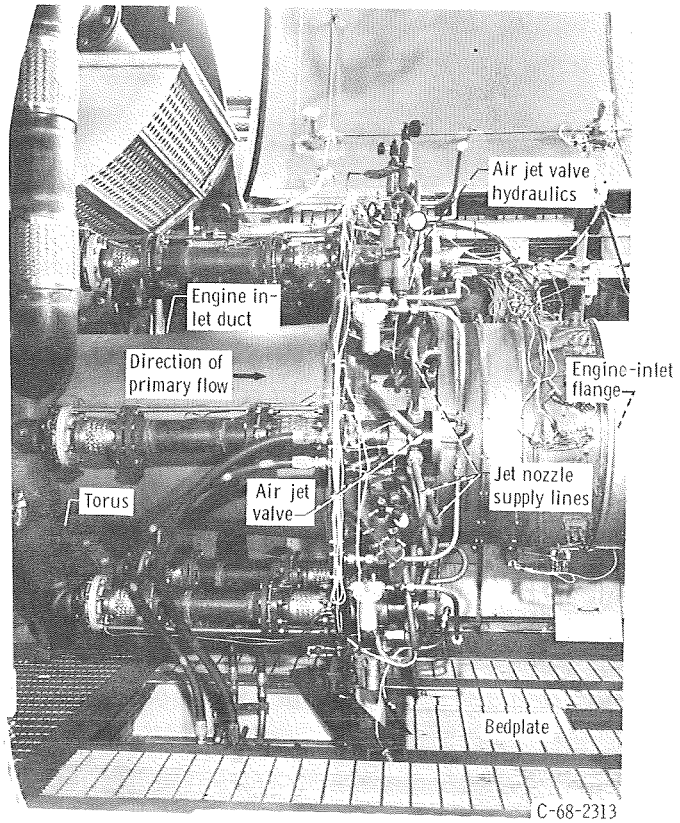

(c) Air jet system and engine-inlet duct.

Figure 2. - Air jet system.

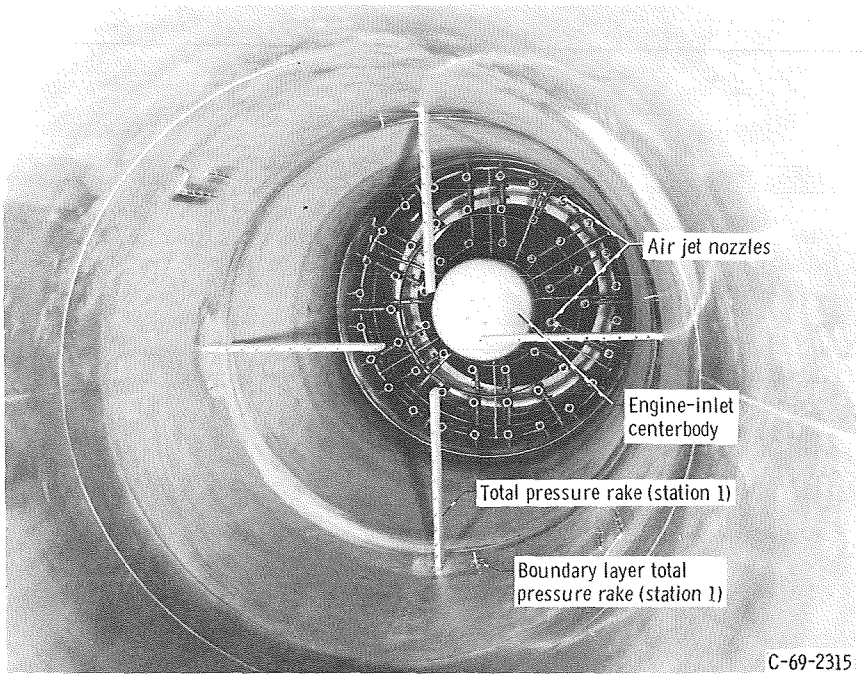

(d) Air jets installed in engine-inlet duct. View looking downstream.
Figure 2. - Concluded.

to control the secondary flow to each 60^{o} segment, were capable of operating up to frequencies of 200 hertz.

Engine and Air Jet System Installation

The air jet system and the engine are shown installed in the Altitude Test Chamber in figure 3. When the air jet system flow (secondary) was shut off, all the engine air was supplied by means of a conventional direct-connect inlet duct. The altitude chamber includes a forward bulkhead which separates the inlet plenum from the test chamber. Conditioned air was supplied to the plenum at the desired pressure and temperature. The chamber aft of the bulkhead was evacuated to the desired altitude pressure. The conditioned air flowed from the plenum through the bellmouth and duct to the engine inlet. When desired, the air jet system introduced high-pressure air (15 to 110 psia or 10.3 to 75.9 N/cm^2 abs) counter to the primary air approximately 36 inches (91.4 cm) upstream of the engine face.

The exhaust from the engine was captured by a collector, extending through the rear bulkhead, to minimize recirculation of the exhaust gases into the test chamber. Constant exhaust pressure was maintained by an automatic control valve.

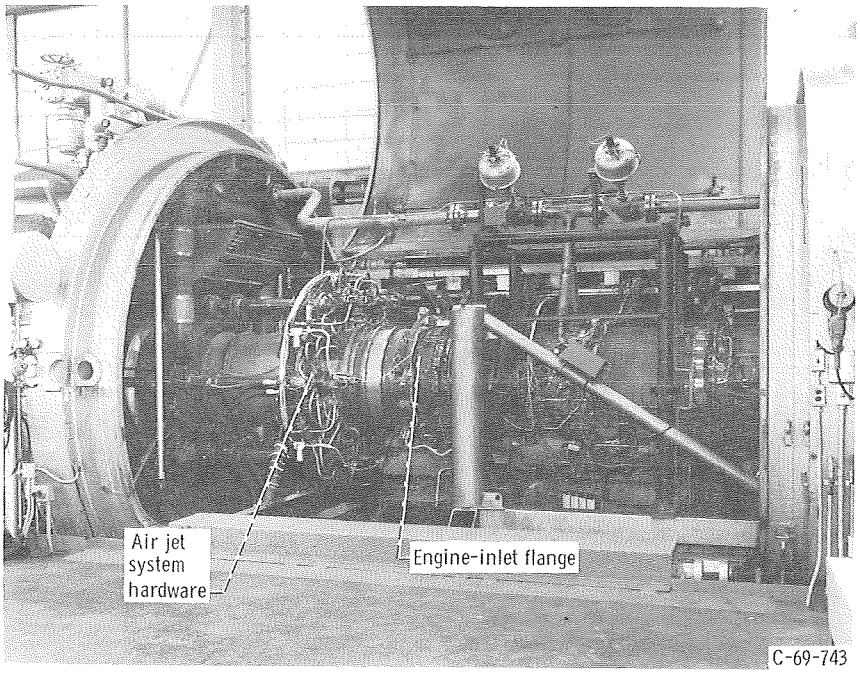

Figure 3. - Turbofan engine and air jet system installed in altitude test chamber.

Instrumentation

The location of the instrumentation is shown for the air jet system in figure 2 and for the engine and inlet duct in figure 4. The station identification and location is shown on the engine schematic (fig. 4), and the location and number of measurements at each station are shown on each station sketch. The station locations were selected to divide the compressor into groups of either three or four stages. Figure 5 shows schematically the circumferential relation between the jets and the engine-inlet total pressure probes. Except for a few select data points, there were 17 transducers located at station 2 as shown in figure 5. For the select data points, transducers were installed in all 40 probes in order to check the instantaneous spatial distortion.

Steady-state. - Pressures were recorded on a digital automatic multiple pressure recorder. Chromel-Alumel thermocouples were used to measure all temperatures and were recorded by means of an automatic voltage digitizer. These systems are described in detail in reference 8.

High-response transient instrumentation. - The locations of the high-response pressure transducers are shown in figures 4 and 5. This instrumentation provided flat frequency response to a minimum of 300 hertz. Typical instrumentation rakes which measure dynamic pressures, as well as steady-state temperatures and pressures, are

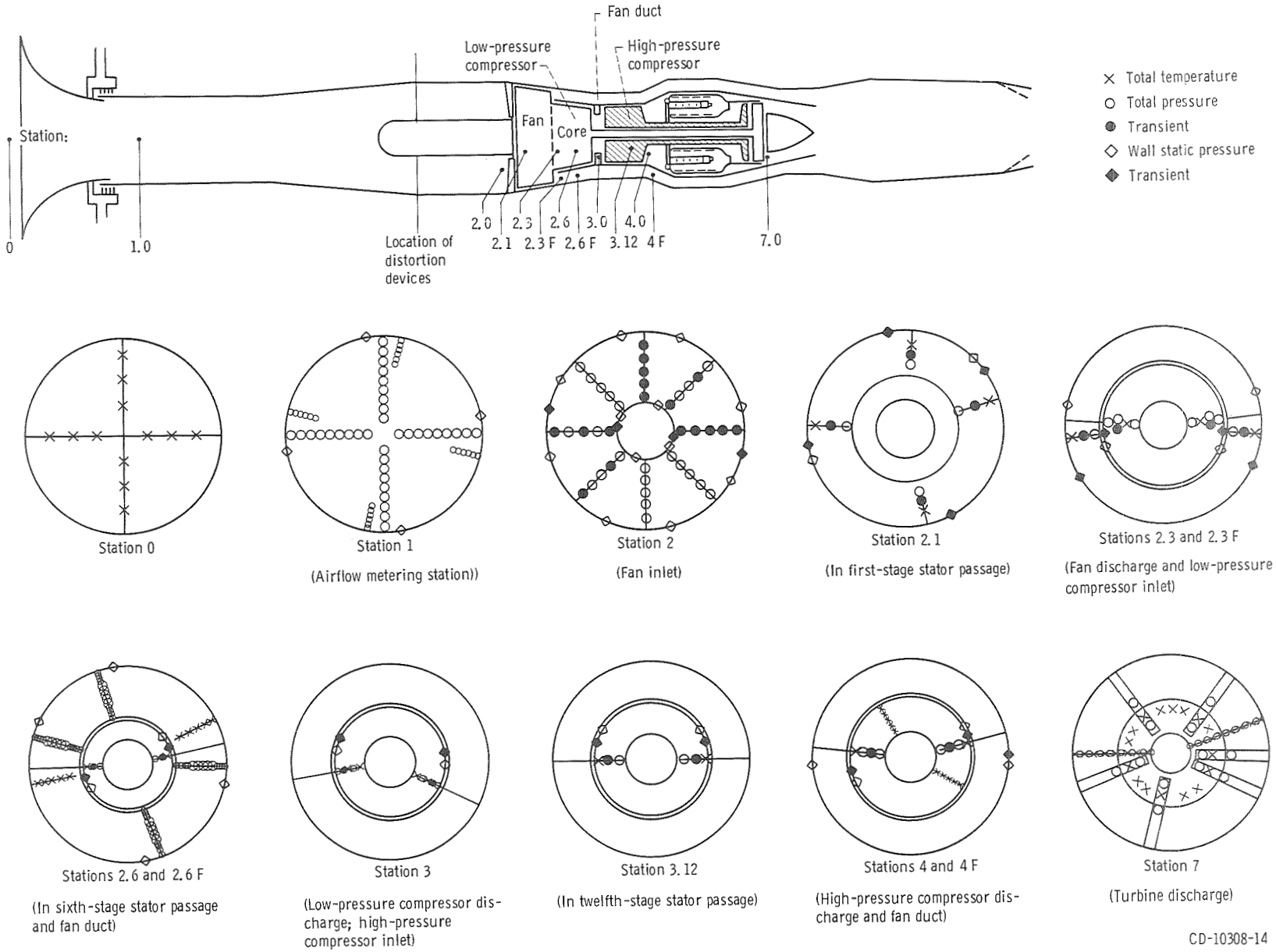

Figure 4. - Instrumentation layout. View looking upstream.

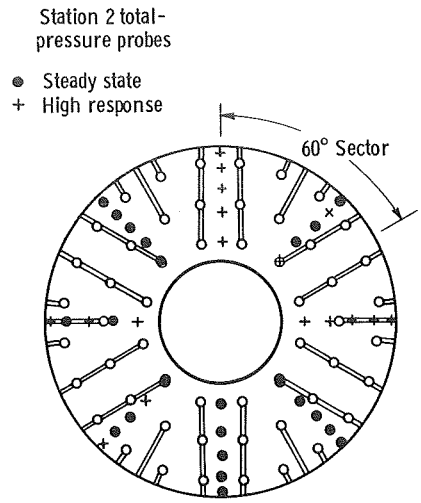

Figure 5. - Spatial relation of engine-inlet (station 2) instrumentation and air jets. View looking upstream.

shown in figure 6. Water cooling of the high-response transducer is illustrate in this figure. The purpose of the water cooling was to maintain the transducer at a temperature below its operational limit. The water cooling also kept the transducer at a near constant temperature so as to minimize its zero and sensitivity change with temperature. A more complete discussion of the use of high-response transducers and the method of calibration just prior to engine-inlet pressure transients is given in reference 9. The high-frequency response data were recorded simultaneously on a high-speed digitizer-recorder (sampling rate of about 50 samples per input per sec) and on magnetic tape which provided both analog and digitized (1000 samples per sec) results.

PROCEDURE

For all test data presented in this report, the engine was stabilized at the desired speed, and the engine-inlet pressure was set at a value that in conjunction with the inlet temperature produced a Reynolds number index of 0.5. (Standard conditions at sea-level static yield a Reynolds number index of 1.0.) During the course of the investigation, the engine-inlet temperature varied between 60° and 90° F (16° and 32° C). Because it was not possible to control the secondary air temperature, the primary air temperature was set approximately equal to the existing secondary air temperature. This was done so as not to introduce a temperature distortion at the engine inlet. The corresponding range of engine-inlet pressures necessary to provide a Reynolds number index of 0.5 was 7.35 to 7.90 psia (5.07 to 5.45 N/cm^2 abs). The engine exhaust pressure was set

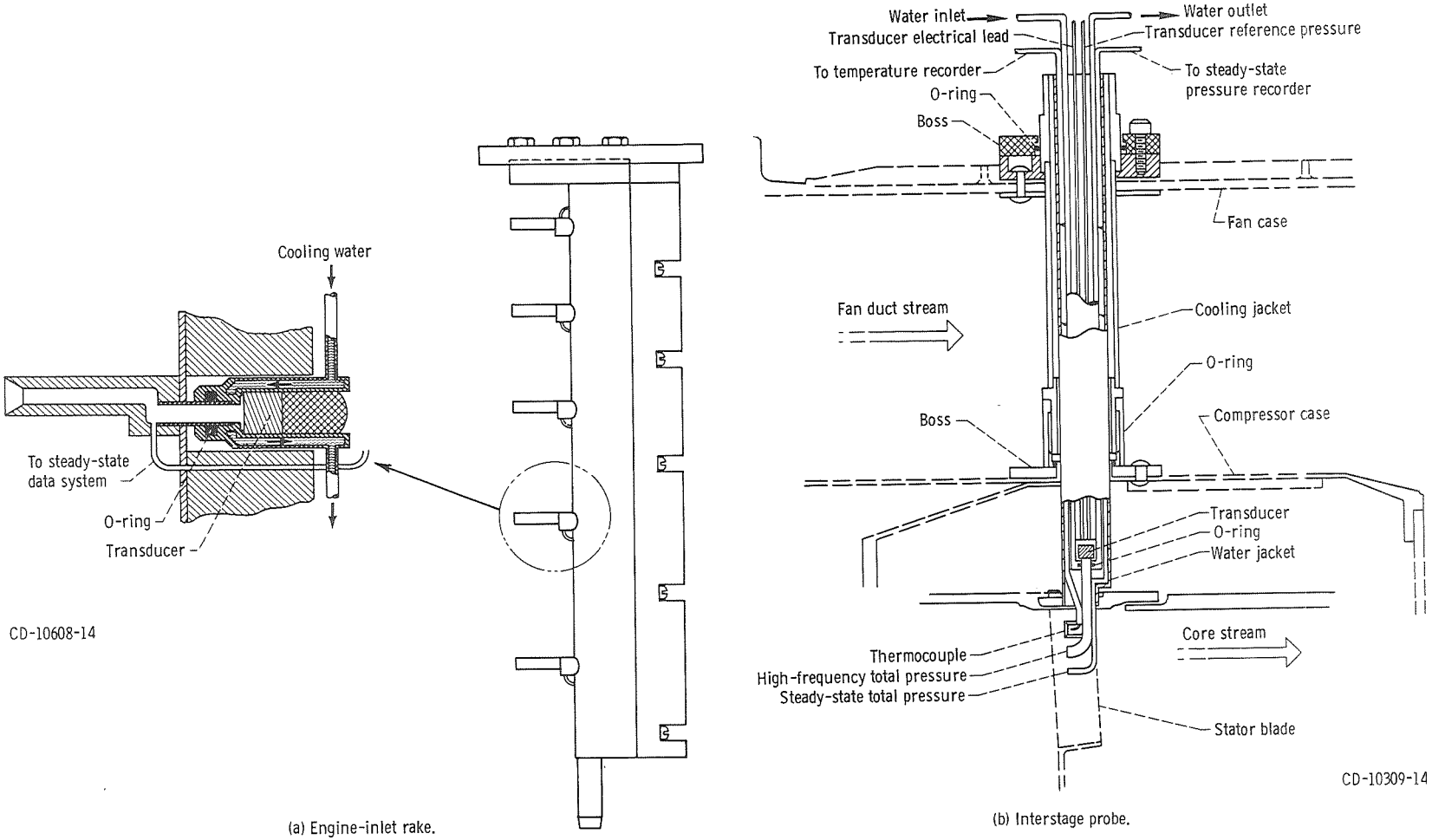

(a) Engine-inlet rake.

(b) Interstage probe.

Figure 6. - Typical rakes.

at 2.4 psia (1.66 N/cm^2 abs) for all tests. In addition, the compressor bleed systems were closed and the engine exhaust nozzle area was maintained at its rated value (i.e., 3.65 ft^2 or 0.339 m^2).

Uniform Oscillations At Discrete Frequencies

The engine and its inlet and exhaust conditions were stabilized at the desired conditions with the air jet (secondary) flow near zero (i.e., upstream gate valve open, upstream butterfly valve closed). The six air jet valves were then adjusted and balanced to produce the desired air jet valve travel. With all secondary air system valves sta-

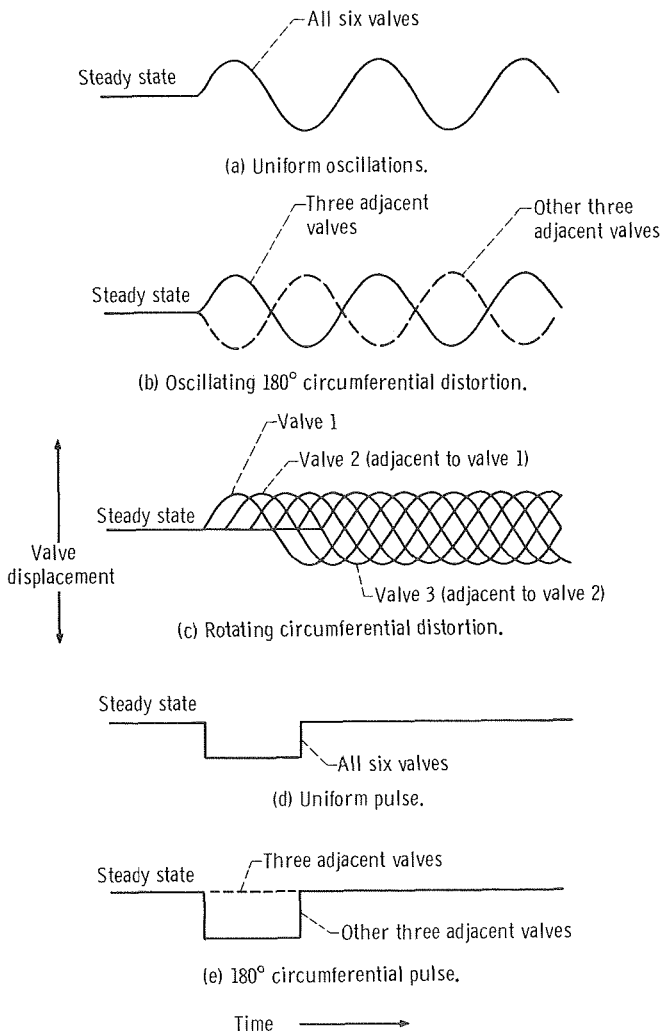

Figure 7. - Air jet valve displacement with time for several types of inlet pressure dynamic testing.

tionary, steady-state data were taken followed by a two-point calibration of the high-response transducers (see ref. 9). Immediately following the transducer calibration, with the analog and digital transient data systems recording, the six air jet valves were activated at the desired frequency and amplitude and the butterfly valve was slowly opened producing a gradual increase in the average air jet system flow. The displacement of the air jet valves with time during this test is shown in figure 7(a). In order to maintain the average engine-inlet pressure constant, it was necessary to adjust a facility primary air valve to compensate for the rising air jet system flow. Increasing the air jet flow and consequently the engine-inlet pressure amplitude was continued until the butterfly valve was fully open or compressor stall occurred.

Uniform Oscillations During A Frequency Sweep

For these tests, the air jet valves were driven by a sweep frequency generator. With the butterfly valve closed, the six air jet valves were adjusted and balanced to produce the desired travel as before. Then with the valves stationary and set at the midpoint of their desired travel, the butterfly valve was gradually open to its maximum position and the desired engine-inlet pressure produced by proper adjustment of the facility primary air supply valve. With the engine stabilized, the steady-state and calibration data were taken as before. Then with the transient data systems operating the frequency generator was activated at 1 hertz and the frequency slowly increased to 140 hertz or until compressor stall occurred. If compressor stall was encountered prior to reaching the 140 hertz, the procedure was to activate the air jet valves at 140 hertz with the butterfly valve closed following the steady-state and calibration data; then, with the transient data systems operating, open the butterfly valve to full open while maintaining constant average engine-inlet pressure. Following this, the frequency sweep generator would slowly reduce air jet valve frequency until compressor stall occurred.

Oscillating 180° Circumferential Distortion At Discrete Frequencies

For this test three adjacent air jet valves on one side of the engine-inlet duct were operated 180° out of phase with the other three valves. The phasing of the valves was accomplished through the use of an analog computer from the moment they were activated. Following the adjusting and balancing of the six air jet valves with the butterfly valve closed, and with the valves set at the midpoint of their travel, the butterfly valve was opened and the engine and its inlet and exhaust conditions stabilized at their desired

levels. The steady-state and calibration data were then taken, and with the transient data systems recording, the computer activated the air jet valves and gradually increased the valve amplitude until the maximum preset valve amplitudes were reached or compressor stall occurred. Figure 7(b) describes the air jet valve displacement during this test.

Rotating Circumferential Distortion At Discrete Frequencies

The procedure used for this test was identical to that used for the "oscillating 180°" test except that each air jet valve was 60° out of phase with the adjacent valve. The rate of rotation in revolutions per second of the low engine-inlet pressure region in either direction was equal to that of the imposed input frequency. The air jet valve displacement for this test is shown in figure 7(c).

Single Inlet Pressure Pulses

For this test, all air jet valves were closed with the butterfly valve open. Following the acquisition of the steady-state and calibration data, an analog computer was used to

TABLE I. - SUMMARY OF INLET DYNAMIC TESTS

Type of test	Method of amplitude variation		Valve input	Frequency, Hz	Number of engine speeds
	Valve	Supply pressure			
Uniform oscillations at discrete frequencies	Constant (maximum)	Zero to maximum (or stall)	Sine wave	9 discrete frequencies: 1 to 200	4
Uniform oscillations during a frequency sweep	Constant	3 levels	Sine wave	1 to 140	1
Oscillating 180° circumferential distortion at discrete frequency	Up to maximum (or stall)	Maximum	Sine wave	10 discrete frequencies: 1 to 200	2
Rotating circumferential distortion at discrete frequencies[a]	Up to maximum (or stall)	Maximum	Sine wave	[b]8 discrete frequencies: 1 to 140	1
Single-inlet pressure pulses[c]	Up to maximum (or stall)	Maximum	Square pulse	----------	2

[a]Low-pressure region corotated and contrarotated with the compressor rotors.
[b]Emphasized frequencies near one-half of fan rotor speed.
[c]Pulse time varied from 5 to 1000 msec; circumferential extent of 180° and 360°.

produce a programmed step of the air jet valves. Figures 7(d) and (e) illustrate the air jet valve displacement during the pulse test. The size of the valve step was increased in small increments until maximum valve travel or compressor stall was encountered. The pulse durations were also varied from 5 to 1000 milliseconds and, in addition, the number of air jet valves, which were stepped, varied from one (60° circumferential extent) to six (360° circumferential extent). Only data obtained for 180° and 360° extent are presented in this report. A more comprehensive presentation of all the pulse data is presented in reference 10. A summary of the previously described dynamic tests is presented in table I.

Data Processing

Steady-state data were obtained to provide a base point for the transient data. The two-point calibration taken before each transient in conjunction with the steady-state data provided the information necessary to calculate the local instantaneous levels of pressure. The transient analog data were available as time histories and are present in this form for a few representative cases. Short time spans of this data were also digitized, generally at 1-millisecond intervals, so that calculated results could be more readily obtained and plotted.

RESULTS AND DISCUSSION

Air Jet System Capability in Producing Engine-Inlet Pressure Variations

The purpose of the discussion and data presented in this section of the report is to exhibit the various patterns of engine-inlet pressure variations that were generated with the air jet system. A more complete and fundamental presentation of the air jet system performance can be found in references 6 and 7.

Normalized engine-inlet total pressure amplitude $\left(P_{T,2_{max}} - P_{T,2_{min}}\right)/P_{T,2_{ss}}$ is shown as a function of input frequency in figure 8 to illustrate the dynamic response of the engine-inlet pressure over a range of frequencies from 1 to 140 hertz. (Symbols are defined in the appendix.) The steady-state pressure was used in the calculation of normalized amplitude instead of the average between $P_{T,2_{max}}$ and $P_{T,2_{min}}$ because it gives nearly the same result and was more convenient to use. These data were obtained at a constant air jet system supply pressure and with all six air jet valves operating in phase at the same amplitude. The steady-state values of engine-inlet pressure and corrected air flow were 7.74 psia (5.34 N/cm^2 abs) and 220 pounds per second

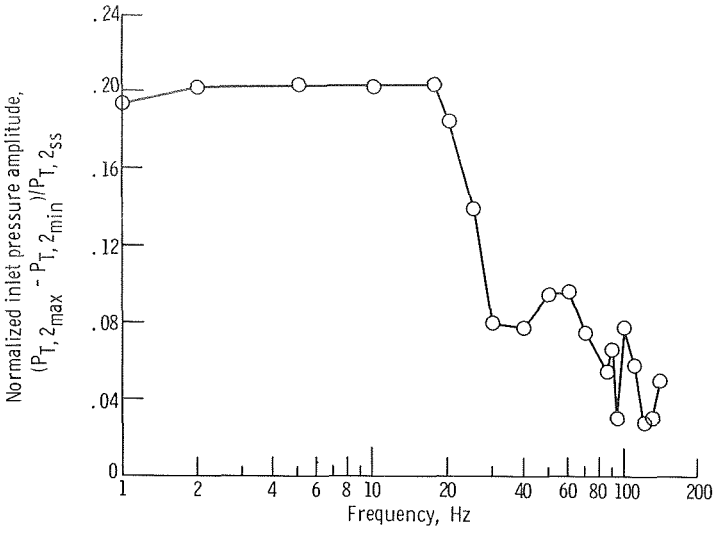

Figure 8. - Typical variation of normalized engine-inlet pressure amplitude with frequency. Engine corrected air flow, 220 pounds per second, (99.6 kg/sec), steady-state inlet total pressure, 7.74 psia (5.34 N/cm^2 abs).

(99.6 kg/sec). The data of figure 8 represent operation at a valve amplitude and air jet supply pressure (flow) less than maximum, so that a complete frequency spectrum can be shown without interruption due to compressor stall. Consequently, the engine-inlet pressure amplitudes do not represent the maximum obtainable.

The most significant trend is the rapid attenuation in amplitude above 20 hertz. This attenuation is associated with the air jet system supply-line dynamics upstream and downstream of the air jet valves and the dynamic characteristics of the engine-inlet duct. A study of these factors and possible methods to reduce the attenuation at the higher frequencies is presented in reference 7. As a result of the low inlet pressure amplitudes obtained at input frequencies over 80 hertz, along with the attenuation of the pressure amplitudes through the compressor system, subsequent data presented in this report are only shown up to a frequency of 80 hertz even though the air jet valve capability was as high as 200 hertz.

The ability of the air jet system to produced engine-inlet pressure oscillations without introducing sizable instantaneous distortions is presented in figure 9. Inlet pressure is plotted as a function of time for a pressure oscillation imposed at 10 hertz. The data used to construct this figure were measured at 40 spatially different locations at the inlet (see fig. 5 for the probe locations and their relation to the air jet hardware). (In any given time region in fig. 9, 40 points are not shown because of pressure-time duplication and five probe locations producing erroneous measurements). The envelope curves of

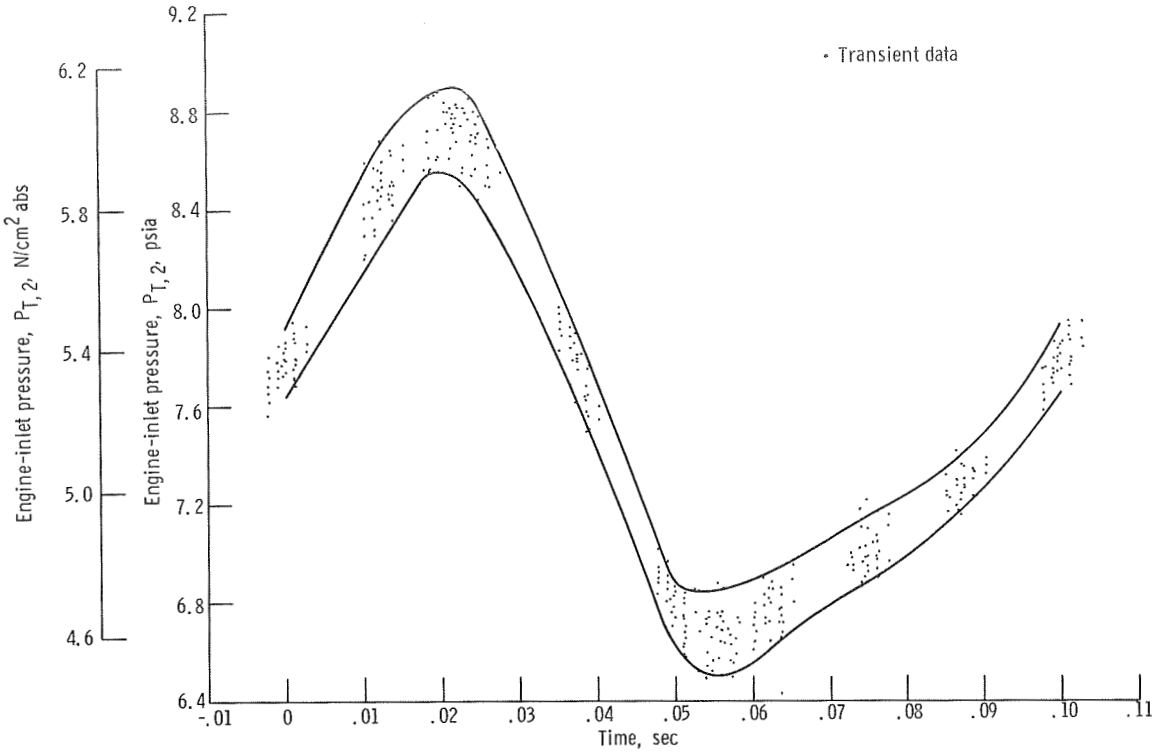

Figure 9. - Typical variation of engine-inlet pressure during uniform cyclic pressure oscillation. Input frequency, 10 hertz.

figure 9 were used to calculate the instantaneous spatial distortion at twelve different times during the cycle. The distortion parameter used was $\left(P_{T,2_{avg}} - P_{T,2_{min}}\right)/P_{T,2_{avg}}$. The results of this calculation along with that obtained for the steady-state condition with a clean inlet duct (i.e., no air jet hardware) yielded the following comparison:

	$\left(P_{T,2_{avg}} - P_{T,2_{min}}\right)/P_{T,2_{avg}} \times 100$, percent
Steady state	1.5
During cycle	
Average	1.9
Maximum	2.5
Minimum	1.4

If the measurement and readout accuracies of transient data are considered, the agreement illustrated shows that the air jet system can produce engine-inlet pressure oscillations without any substantial increase in instantaneous spatial distortion level over that obtained during steady-state operation.

Typical engine-inlet total pressure-time histories are presented in figure 10 for three different modes of air jet system operation. In each case the variation with time of two inlet pressures 180^{o} apart are shown. Figure 10(a) exhibits the variation of the two pressures during the uniform cyclic mode at 20 hertz. Figure 10(b) shows how the same pressure measurements changed for the oscillating 180^{o} circumferential distortion at 20 hertz. Figure 10(c) presents the pressure variation when a uniform pulse was imposed at the engine inlet.

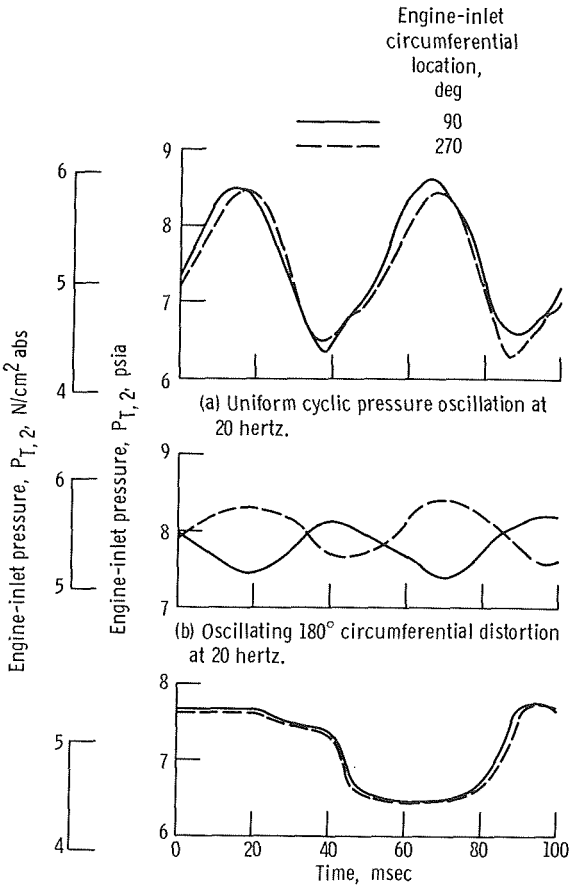

Figure 10. - Typical variation of engine-inlet pressure during air jet operation.

Fan-Compressor Response to Uniform Engine-Inlet Dynamic Pressure Variations

Cyclic oscillations. - Typical time histories of 14 total pressures located throughout the fan-compressor system are presented in figure 11 during a uniform (zero instantaneous distortion) engine-inlet pressure oscillation. These 14 pressures consisted of two pressures (approximately 180^{o} apart; see fig. 4) at each of seven fan-compressor stations (i.e., station 2, 2.3F, 2.3, 2.6, 3, 3.12, and 4). The radical location of each measurement was near or at the midpassage height. As previously stated (see PROCEDURE), the inlet pressure amplitude was gradually increased until limited by air jet system capacity or compressor stall. Figure 11 shows the last pressure cycle at 10 hertz prior to stall and the stall itself. When stall occurred, the nor-

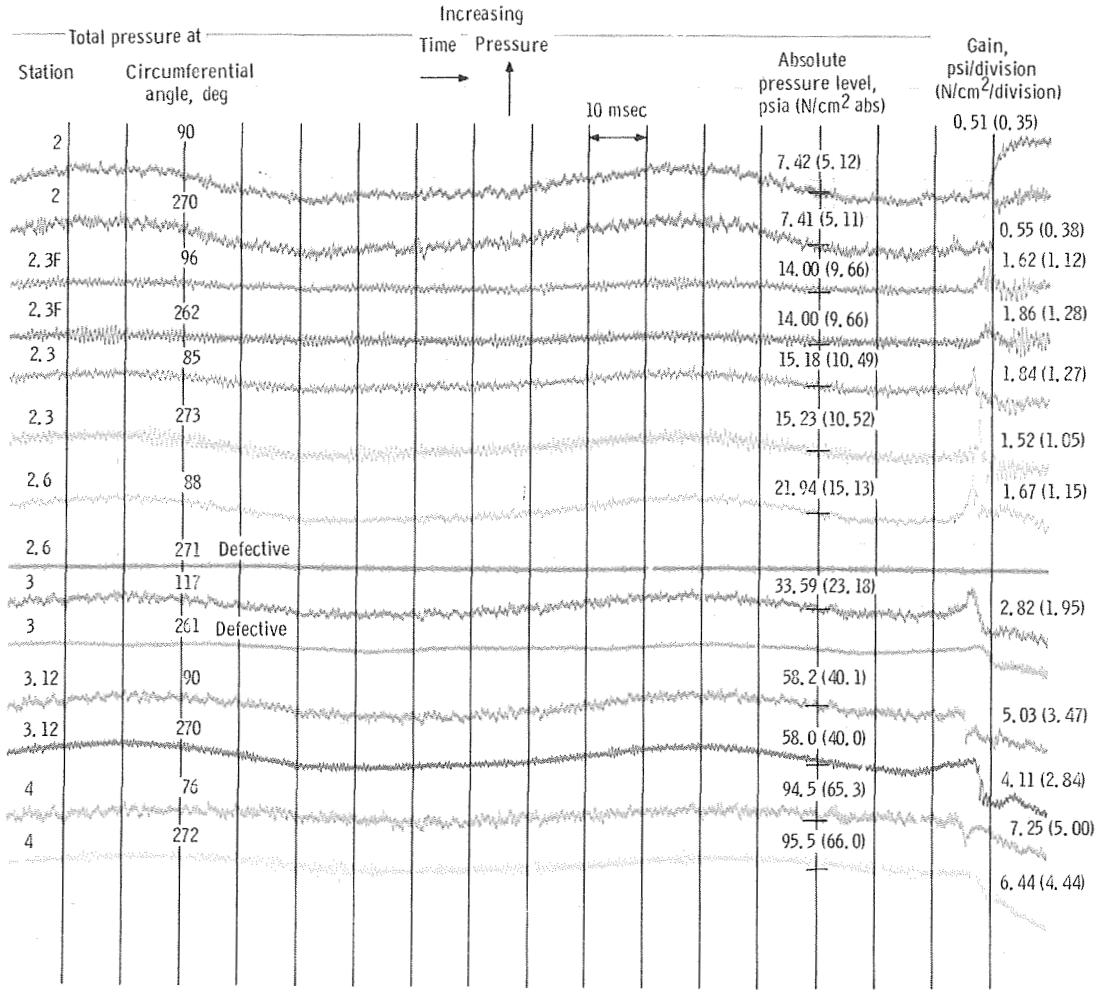

Figure 11. - Typical fan-compressor time histories during 10-hertz uniform engine-inlet cyclic pressure variation leading to stall. High-pressure rotor speed, 13 234 rpm; exhaust nozzle area, 100 percent rated; Reynolds number index, 0.5.

malized inlet pressure amplitude $\left(P_{T,2_{max}} - P_{T,2_{min}}\right)/P_{T,2_{ss}}$ had reached a value of about 0.28. Stall appears to have originated in the high-pressure compressor as evidenced by the fall-off in pressures in this compressor, and the rise (or hammer-shock effect) ahead of the high-pressure compressor. The data also indicate that the flow breakdown in the high-pressure compressor occurs 2 or 3 milliseconds sooner on the right side of the engine (90° circumferential location looking upstream). For the uniform inlet pressure oscillation, the earlier flow breakdown on the right side of the engine occurred repeatedly during many other stall encounters. This sequence also occurred during slow engine accelerations (quasi-steady-state stalls encountered without distortion but with nozzle areas other than rated). Other characteristics which are exhibited by the data of figure 11 are the phase shift through the compressor and the differences in both pressure and normalized pressure amplitude for the various fan-compressor stations. The phase shift (lag) is about 10 milliseconds from station 2 (fan-compressor inlet) to station 4 (high-pressure compressor exit). The attenuation of the normalized pressure amplitudes for the various fan-compressor stations is discernible from figure 11 but is quantitatively illustrated and summarized for a range of frequencies in figure 12.

Figure 12 shows the variation of pressure amplitude for several fan-compressor stations over a range of input frequencies. Figure 12(a) presents the normalized amplitude. The trend exhibited by the engine-inlet pressure data are consistent with the data previously shown in figure 8 which illustrated the air jet system limitations as frequency is increased. Figure 12(b) shows the normalized amplitude ratio which is the data of figure 12(a) divided by the normalized amplitude at station 2. The normalized amplitudes for the locations within the fan compressor decrease with frequency from 1 to 30 or 40 hertz, and then increase as frequency is increased to 80 hertz. The normalized amplitudes for the downstream stations of the compressor (stations 3.12 and 4) and the fan exit (station 2.3 F) show the greatest attenuation. The attenuation at the high-pressure compressor exit (station 4) is such that when the input frequency is raised to 30 hertz and above, no measurable pressure amplitudes were evident. It is necessary to add, however, that the low input pressure amplitude at the engine inlet above 20 hertz and use of transducers with a necessarily high range at the compressor exit may well have influenced this result.

The phase shift through the compressor system is summarized in figure 13 where phase shift in degrees is plotted as a function of input frequency. These data show that, for all stations in the fan-compressor system, the phase shift increases with frequency; and at a given frequency, with the possible exception of the fan exit (station 2.3 F), the phase shift is greater as the flow moves through the compressor. The effect of the amplitude ratio and phase shift variations shown by the data of figures 12 and 13 are to produce a time variant change in the stage group pressure ratios as uniform inlet pres-

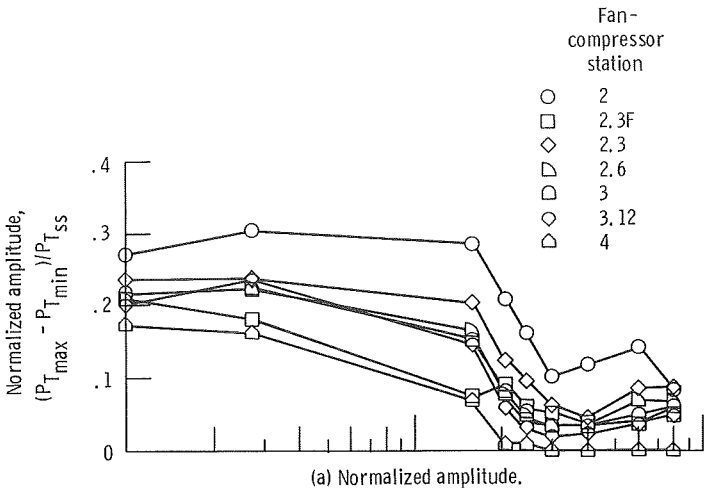

(a) Normalized amplitude.

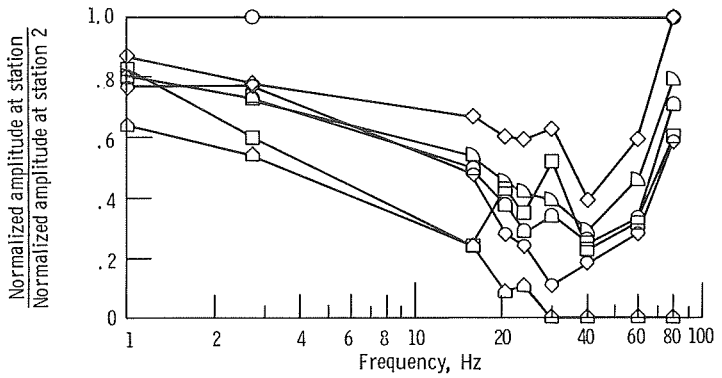

(b) Normalized amplitude ratio.

Figure 12. - Dynamic response of compressor system during uniform inlet pressure oscillations. High-pressure rotor speed, 13 350 rpm; exhaust nozzle area, 100 percent rated; Reynolds number index, 0.5.

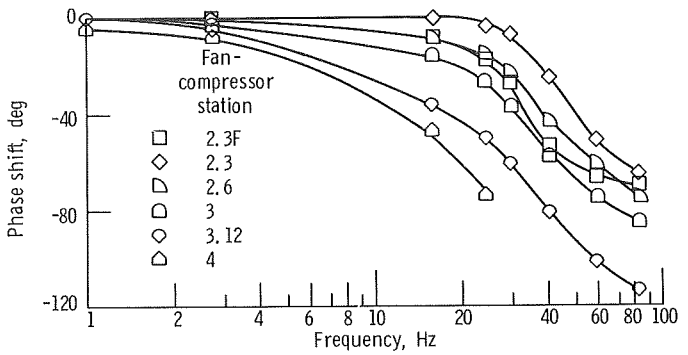

Figure 13. - Phase shift relative to station 2 (engine inlet) at various fan-compressor stations during uniform inlet pressure oscillations. High-pressure rotor speed, 13 350 rpm; exhaust nozzle area, 100 percent rated; Reynolds number index, 0.5.

sure oscillations are imposed at the fan-compressor inlet. The next two figures are presented to demonstrate the effects of inlet pressure amplitude and frequency on the stage group pressure ratios.

The data of figure 11 (frequency of 10 Hz), were used to calculate the stage group pressure ratios up to the time of flow breakdown. The results are displayed in figure 14 in coordinates of pressure ratio and time. The maximum pressure ratio swings were exhibited by the fan tip, fan hub, and high-compressor rear stage groups. The data also show that the average pressure ratio (as determined from the maximum and minimum) differ substantially from the steady-state value (established prior to the inlet oscillation) in the case of the high-pressure compressor. The front stage group of this compressor (3.12/3) remains at or below its steady-state value during the imposed pressure oscillation, while the rear stage group (4/3.12) has an average pressure ratio well above its steady-state value. Matching the time at which events occur using the

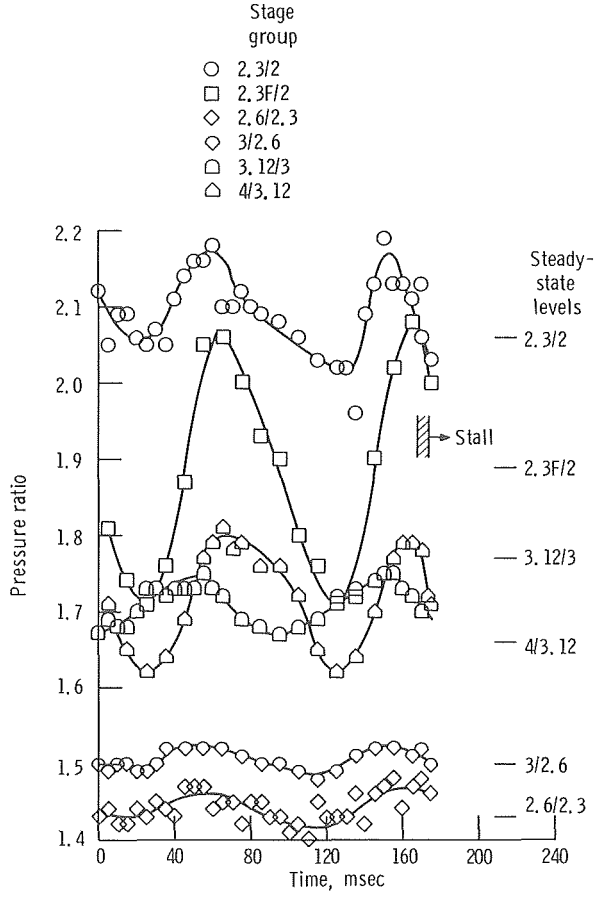

Figure 14. - Typical fan-compressor stage group pressure ratios during uniform engine-inlet cyclic pressure variation at 10 hertz. High-pressure rotor speed, 13 234 rpm; exhaust nozzle area, 100 percent rated; Reynolds number index, 0.5.

data presented in figures 11 and 14 shows that the stage group pressure ratios are at or near their respective peak values, when the inlet pressure is at the lowest level of the imposed oscillation. Thus with instantaneous inlet spatial distortion levels equivalent to those encountered during clean inlet testing, rapid changes in inlet pressure produced conditions in the fan-compressor associated with stall, namely, pressure ratios well above the steady-state operating valves.

The data of figure 14 and similar data at other inlet pressure frequencies were used to calculate the ratio of peak pressure ratio to steady-state pressure ratio for each stage group. This was done for two levels of normalized inlet pressure amplitude $\left(P_{T,2_{max}} - P_{T,2_{min}}\right)/P_{T,2_{ss}}$, 0.27 and 0.09. The reason for selecting the lower value of normalized amplitude was to permit the previous calculation to be made for frequencies above 20 hertz where values above 0.09 could not be consistently attained (see fig. 12(a)). The results are plotted in figure 15 where the ratio of peak to steady-state pressure ratio for each stage group is shown over a range of frequencies.

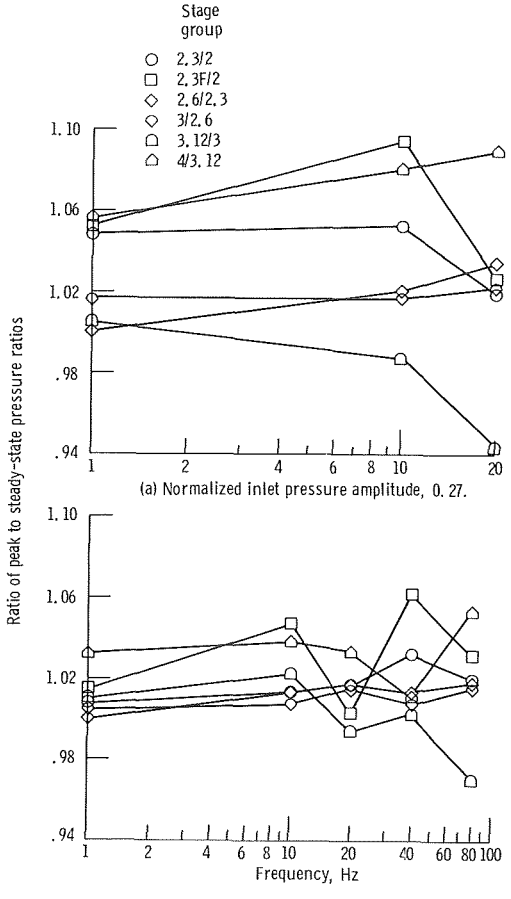

(a) Normalized inlet pressure amplitude, 0.27.

(b) Normalized inlet pressure amplitude, 0.09.

Figure 15. - Variation of peak stage group pressure ratios with frequency. High-pressure rotor speed; 13 230 rpm; exhaust nozzle area, 100 percent rated; Reynolds number index, 0.5.

The data show that, for a given inlet pressure input amplitude, the peak pressure ratios vary substantially as frequency is varied over the range of 1 to 80 hertz. Thus the input amplitude required to stall the fan-compressor system might be expected to vary as frequency is changed. Unfortunately, because of the limitations in the air jet system above 20 hertz, a thorough verification of the aforementioned was not possible.

The data taken during the uniform inlet pressure frequency sweeps and at discrete frequencies (see PROCEDURE), were used to construct figure 16 on coordinates of nor-

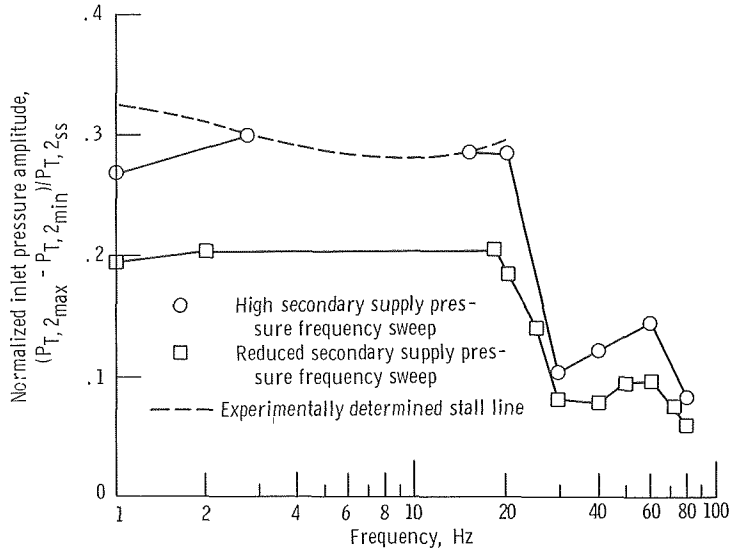

Figure 16. - Stall limit and operating characteristics during uniform engine-inlet cyclic pressure variations on coordinates of normalized inlet pressure amplitude and input frequency. High-pressure rotor speed, 13 300 rpm; exhaust nozzle area, 100 percent rated; Reynolds number index, 0.5.

malized inlet pressure amplitude and frequency. The two curves designated as "frequency sweeps" were obtained by operating the air jet valves near maximum amplitude at two levels of supply pressure. At the lower supply pressure, a frequency sweep was made from 1 to 140 hertz (fig. 16 only shows data to 80 Hz) without encountering stall. At the higher supply pressure, stall was encountered at 2.7 hertz as frequency was increased and at 15.2 hertz as frequency was decreased. In addition, stall points were obtained during discrete frequency testing at frequencies from 1 to 20 hertz. (During discrete frequency testing, slightly higher inlet pressure amplitudes were obtained due to the availability of a slightly higher air jet supply pressure.) Over the frequency range from 1 to 20 hertz, the normalized inlet pressure amplitude required to produce stall was maximum at about 0.33 at 1 hertz and a minimum of 0.28 at 10 hertz.

Single pulse. - Typical time histories of 14 pressures located throughout the fan-compressor system are presented in figure 17, while uniform engine-inlet pressure pulses were being introduced. As previously stated (see PROCEDURE), inlet pressure amplitude was successively increased until limited by air jet system capability or compressor stall. Figure 17 shows data for two inlet pressure pulses - one not quite large enough to produce stall and one which did produce stall. The time histories of the fan-compressor pressures at stall for the single pulse mode looks quite similar to that previously shown for the cyclic oscillations (fig. 11). Stall as before appears to have originated in the high-pressure compressor. Again, flow breakdown first occurred on the right side of the compressor.

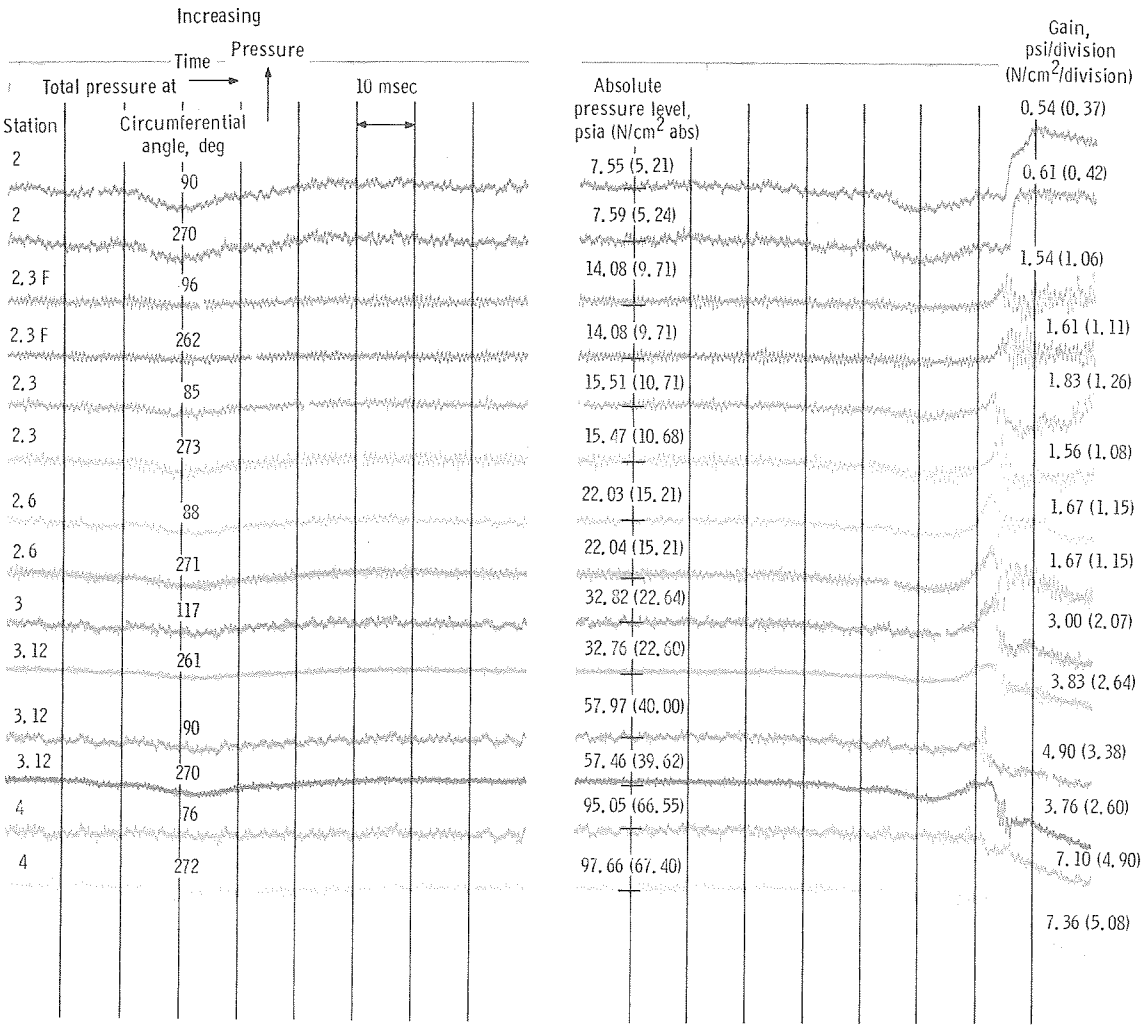

(a) Pulse without stall.

(b) Increased amplitude pulse with stall.

Figure 17. - Typical fan-compressor time histories during uniform engine-inlet single pressure pulse. Air jet valve pulse time, 13 milliseconds; high-pressure rotor speed, 13 235 rpm; exhaust nozzle area, 100 percent rated; Reynolds number index, 0.5.

The data of figure 17 were used to calculate the stage group pressure ratios up to the time of flow breakdown. The variation of these stage group pressure ratios with time are presented in figure 18. Here again, the maximum deviation of stage group pressure ratios from their respective steady-state values is exhibited by the fan tip, fan hub, and high-compressor rear stage groups. It is of interest to note that the maximum pressure ratios attained during the single pulse test prior to stall are similar for all stage groups to those encountered prior to stall with the cyclic oscillation.

One other point of comparison between the uniform cyclic and pulse inlet pressure variation is worthy of note. As was stated previously for frequencies from 1 to 20 hertz, the magnitude of the normalized inlet pressure amplitude $\left(P_{T,2_{max}} - P_{T,2_{min}}\right)/P_{T,2_{ss}}$ required to stall the fan-compressor system during the cyclic mode was between 0.28 and 0.33. For the pulse mode, the stall value of $\left(P_{T,2_{max}} - P_{T,2_{min}}\right)/P_{T,2_{ss}}$ was

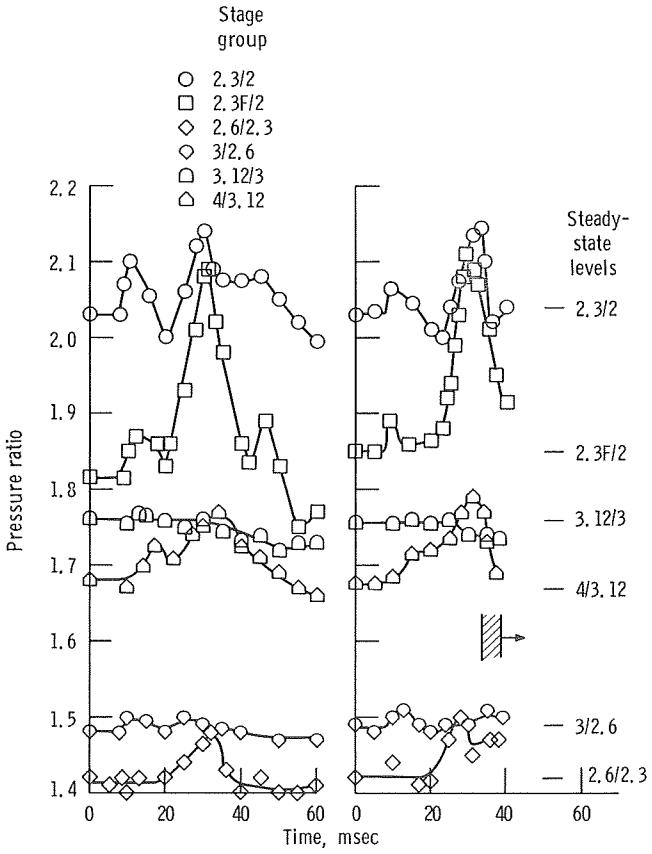

(a) Pulse without stall. (b) Increased amplitude pulse with stall.

Figure 18. - Typical fan-compressor stage group pressure ratios during uniform engine-inlet single pressure pulses. Air jet valve pulse time, 13 milliseconds; high-pressure rotor speed, 13 250 rpm; exhaust nozzle area, 100 percent rated; Reynolds number index, 0.5.

about 0.16 based on the data from figure 17 and other similar data. Previously it was noted, when discussing the uniform cyclic variations in inlet pressure, a decreasing value of inlet pressure resulted in the stage group pressure ratios increasing and thus producing conditions conducive to stall. Conversely, an increasing value of inlet pressure reduced the stage group pressure ratios and thereby moved the fan compressor away from stall. If then a parameter were devised which might better account for only the decreasing inlet pressure, a more accurate comparison between the cyclic and pulse modes could be made. $\left(P_{T,2_{ss}} - P_{T',2_{min}}\right)/P_{T,2_{ss}}$ is such a parameter. $P_{T',2_{min}}$ is defined in this instance as the minimum inlet pressure which occurred prior to stall over at least a 2-millisecond time period. (The reason for selecting a 2-sec time period will be given subsequently.) When this parameter is used, the pulse mode yields the same value at stall as before, namely, 0.16. For the cyclic mode, the value of this parameter varied from about 0.16 to 0.14 depending on the frequency.

Fan-Compressor Response to Distorted Engine-Inlet Dynamic Variations

Typical time histories of 14 pressures located throughout the fan-compressor system are presented in figures 19 and 20 during spatially distorted engine-inlet pressure variations. Figure 19 shows the last three pressure cycles of an oscillating 180° circumferential distortion of 20 hertz leading to stall. Figure 20 shows two 180° circumferential inlet pressure pulses - one without and one with stall. Characteristics of the stall are similar to those illustrated in figures 11 and 17 for the uniform inlet pressure mode. The significant difference between the uniform and distorted inlet tests can readily be seen by comparing the amplitude of the inlet pressure required to produce stall (e.g., figs. 11 and 19; figs. 17 and 20). Comparison of these data shows that the inlet pressure amplitude required to produce stall are substantially less when an instantaneous distortion is present.

In order to summarize and compare the effects of various modes of distortions on the engine stall limits, the results are presented in figure 21 on coordinates of stall tolerance parameter, $\left(P_{T',2_{avg}} - P_{T',2_{min}}\right)/P_{T',2_{avg}}$, and input frequency. $P_{T',2_{avg}}$ is defined as the average pressure between $P_{T',2_{max}}$ and $P_{T',2_{min}}$. $P_{T',2_{max}}$ and $P_{T',2_{min}}$ are the maximum and minimum inlet pressures which occurred prior to stall over at least a 2-millisecond time period. The 2-millisecond time period was selected as significant because it represents the approximate time for the fan-low compressor to rotate 90° at rotor speed for which the data are shown. Stall margin is relatively insensitive to circumferential distortion extent above 90° while at values well below 90°

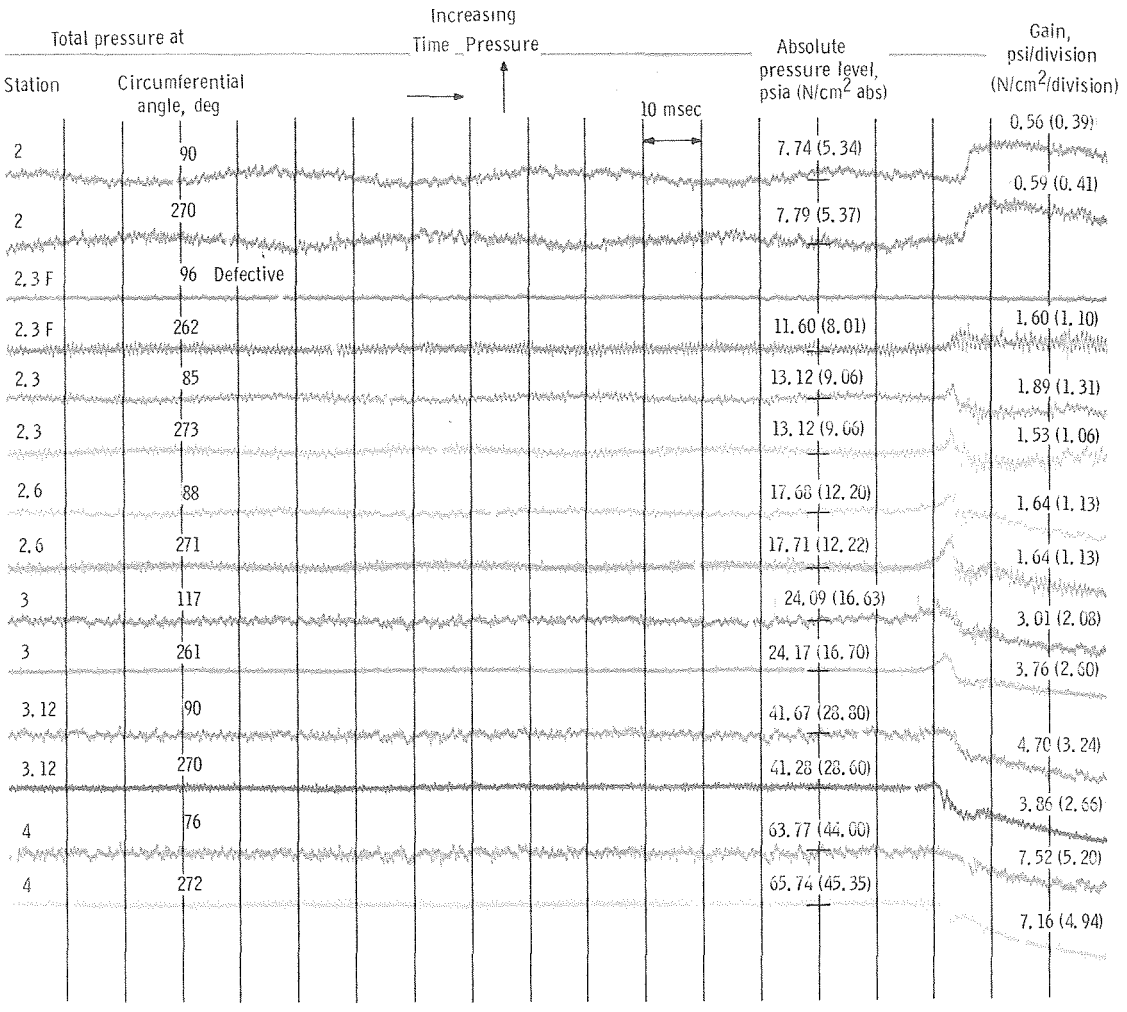

Figure 19. - Typical fan-compressor time histories during 20-hertz 180° out-of-phase engine-inlet cyclic pressure variation leading to stall. High-pressure rotor speed, 12 194 rpm; exhaust nozzle area, 100 percent rated; Reynolds number index, 0.5.

substantially greater distortions without producing stall are possible. For those modes of distortion not related to frequency, namely, steady-state and 180^{o} pulse, the levels of stall tolerance parameter at stall are merely indicated on the ordinate of the figure. For the oscillating 180^{o} and the rotating distortions, the results are plotted at their appropriate frequencies. Stall tolerance parameter is defined in this manner for the distorted inlet pressure data because the resulting parameter is a measure of the instantaneous distortion (subject, of course, to the 2-msec criteria). Thus, if instantaneous distortion were the sole factor in determining stall, all modes and frequencies of inlet pressure varaiations should produce stall at the same value of stall tolerance parameter.

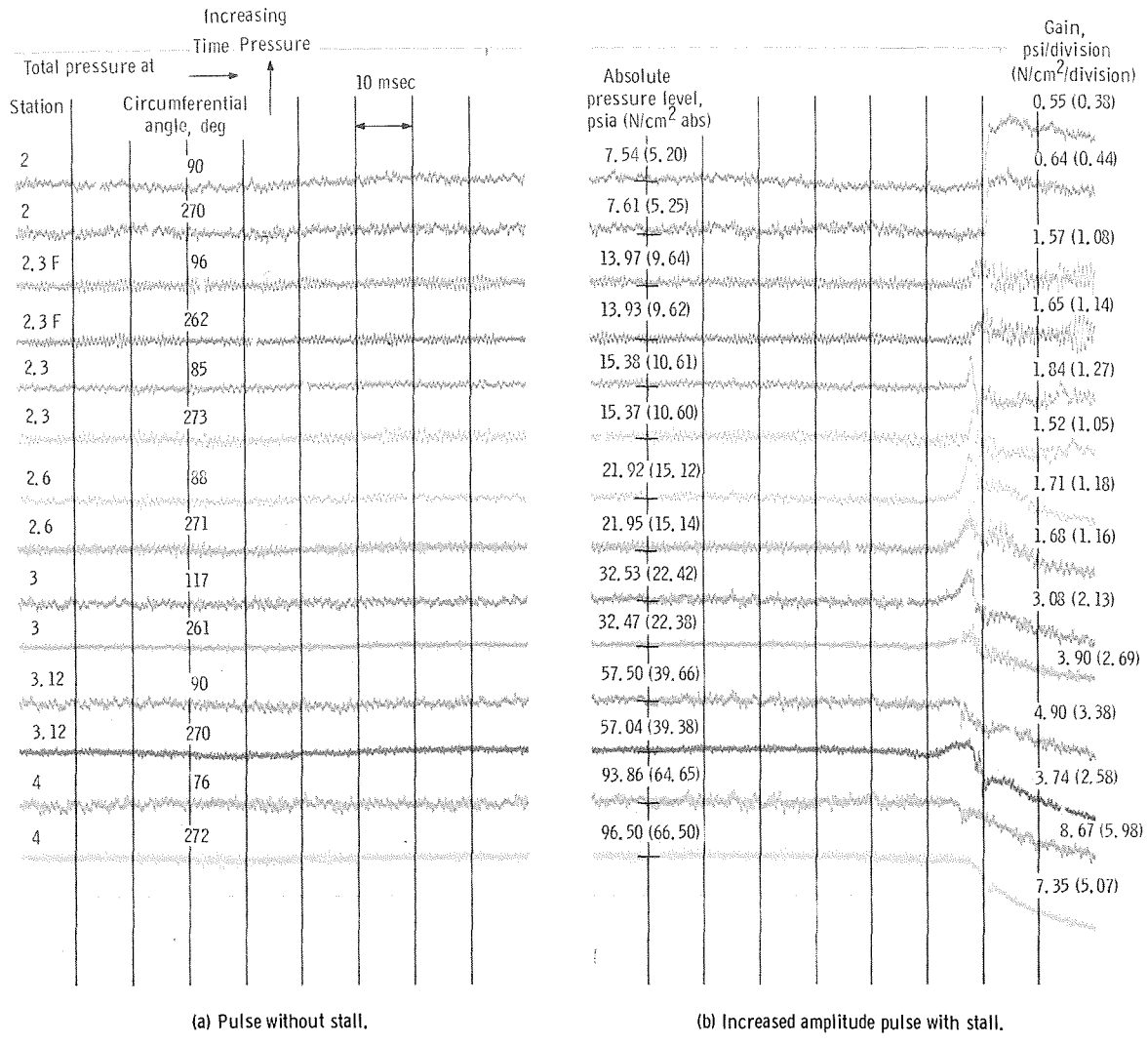

(a) Pulse without stall.

(b) Increased amplitude pulse with stall.

Figure 20. - Typical fan-compressor time histories during 180° engine-inlet single pressure pulse. Air jet valve pulse time, 15 milliseconds; high-pressure rotor speed, 13 257 rpm; exhaust nozzle area, 100 percent rated; Reynolds number index, 0.5.

The data presented in figure 21 have been subdivided into two parts. Figure 21(a) compares the stall tolerance parameter for the 180° steady-state distortion, the 180° pulse distortion and the 180° oscillating distortion. Stall was encountered at a stall tolerance parameter of 0.054 with the steady-state distortion as compared to 0.036 when the pulse distortion was imposed. The steady-state value is based on results shown in reference 9. The oscillating distortion produced some variation in stall tolerance parameter as frequency was varied. At 1 hertz the value was 0.073 and it decreased as frequency was raised until a stall tolerance parameter of 0.057 was reached at a frequency of 60 hertz.

Figure 21(b) compares the stall tolerance parameter for the 180° steady-state distortion and the two rotating distortions. When the distortion was contrarotated (opposite

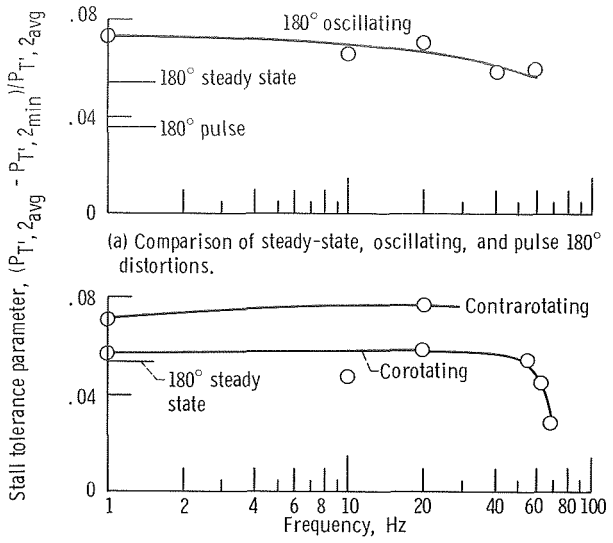

(a) Comparison of steady-state, oscillating, and pulse 180° distortions.

(b) Comparison of rotating and 180° steady-state distortions.

Figure 21. - Effect of several engine-inlet distortion modes on compressor system stall tolerance. High-pressure rotor speed, 13 100 rpm; exhaust nozzle area, 100 percent rated; Reynolds number index, 0.5.

to the direction of the fan-low compressor rotor), the stall tolerance parameter was substantially greater than for the steady-state distortion or the corotating distortion. At 20 hertz the contrarotating value of stall tolerance parameter was 0.078 as compared to 0.059 for the corotating distortion. The steady-state distortion value as previously stated was 0.054. As the frequency of the corotating distortion was increased, the stall tolerance decreased. As the frequency approached 72 hertz (i.e., one-half of fan-low compressor rotor speed), the stall tolerance parameter decreased to about 0.030 which is slightly below the value attained for the 180^{o} pulse distortion. This substantial decrease in stall tolerance parameter with frequency strongly suggests that stall tolerance is a function of the dwell-time of the fan-compressor rotor blading in the low pressure region of an engine-inlet distortion. The data presented in figure 21 also indicate that stall tolerance is related to the rate of change of the inlet pressure as well as the instantaneous distortion level.

CONCLUDING REMARKS

Rapid and controlled changes in engine-inlet total pressure were produced by rapid changes in secondary air flow which was injected as many small contrastream jets ahead of the engine. The flexibility of this air jet system made it possible to produce cyclic

and single pulse variations in engine-inlet pressure with uniform (zero instantaneous spatial distortion) and 180° distortion. It was also possible to create rotating circumferential distortions at the engine inlet at frequencies up to about one-half of fan-low compressor rotor speed.

Cyclic or pulse uniform inlet pressure variations resulted in transient changes in the fan-compressor stage group pressure ratios. The pressure ratio changes were largest for the fan tip, fan hub, and high-compressor rear stage groups. When the normalized amplitude of the uniform cyclic oscillations $\left(P_{T,2_{max}} - P_{T,2_{min}}\right)/P_{T,2_{ss}}$ reached values of 0.28 to 0.33, fan-compressor stall occurred over an input frequency range from 1 to 20 hertz. The parameter $\left(P_{T,2_{ss}} - P_{T',2_{min}}\right)/P_{T,2_{ss}}$ was devised to assess the inlet pressure amplitude required to produce stall during different modes of uniform inlet pressure variations. When this parameter was used, the pulse mode required about 0.16 to stall the compressor. For the cyclic mode, the value of this parameter at stall varied from 0.16 to 0.14 depending on inlet pressure input frequency.

Spatially distorted cyclic and pulse inlet pressure variations resulted in compressor stall at substantially lower inlet pressure amplitudes than those required to produce stall with spatially uniform inlet pressure variations. Stall was produced at lower values of circumferential distortion with the 180° pulsed distortions than with the 180° steady-state distortions. A stall tolerance parameter $\left(P_{T',2_{avg}} - P_{T',2_{min}}\right)/P_{T',2_{avg}}$, which is a measure of the instantaneous distortion level, was used to compare the various distortion modes. Stall occurred over a range of stall tolerance parameter values from 0.078 to 0.030 depending on the mode and frequency of the inlet pressure distortion. The various distortion modes included oscillating 180° distortion, rotating distortion, 180° single pulse, and 180° steady-state distortion. The results showed that stall tolerance is a function of not only the instantaneous distortion level, but also the rate of change of the inlet pressure and the dwell-time of the fan-compressor rotor blading in the low-pressure region of an engine-inlet distortion.

Lewis Research Center,
National Aeronautics and Space Administration,
Cleveland, Ohio, May 5, 1970,
720-03.

APPENDIX - SYMBOLS

$P_{T_{max}}$	maximum instantaneous total pressure at appropriate fan-compressor station
$P_{T_{min}}$	minimum instantaneous total pressure at appropriate fan-compressor
$P_{T_{ss}}$	steady-state total pressure at appropriate fan-compressor station prior to inlet pressure transient
$P_{T,2_{avg}}$	average value of engine-inlet total pressure between $P_{T,2_{max}}$ and $P_{T,2_{min}}$
$P_{T',2_{avg}}$	average value of engine-inlet pressure between $P_{T',2_{max}}$ and $P_{T',2_{min}}$
$P_{T,2_{max}}$	maximum instantaneous engine-inlet total pressure
$P_{T',2_{max}}$	maximum engine-inlet total pressure which occurred prior to stall over time period of at least 2 msec
$P_{T,2_{min}}$	minimum instantaneous engine-inlet total pressure
$P_{T',2_{min}}$	minimum engine-inlet total pressure which occurred prior to stall over time period of at least 2 msec
$P_{T,2_{ss}}$	steady-state engine-inlet total pressure prior to inlet pressure transient
$\frac{P_{T_{max}} - P_{T_{min}}}{P_{T_{ss}}}$	normalized amplitude (applicable to any fan-compressor station)
$\frac{\left(\frac{P_{T_{max}} - P_{T_{min}}}{P_{T_{ss}}}\right)}{\left(\frac{P_{T,2_{max}} - P_{T,2_{min}}}{P_{T,2_{ss}}}\right)}$	normalized amplitude ratio

$\frac{P_{T,2_{ss}} - P_{T',2_{min}}}{P_{T',2_{ss}}}$ stall tolerance parameter for uniform inlet pressure variations

$\frac{P_{T',2_{avg}} - P_{T',2_{min}}}{P_{T',2_{avg}}}$ stall tolerance parameter for distorted inlet pressure variations

REFERENCES

1. Harry, David P., III; and Lubick, Robert J.: Inlet-Air Distortion Effects of Stall, Surge, and Acceleration Margin of a Turbojet Engine Equipped with Variable Compressor Inlet Guide Vanes. NACA RM E54K26, 1955.

2. Huntley, S. C.; Sivo, Joseph N.; and Walker, Curtis L.: Effect of Circumferential Total-Pressure Gradients Typical of Single-Inlet Duct Installations on Performance of an Axial-Flow Turbojet Engine. NACA RM E54K26a, 1955.

3. Russey, Robert E.; and Lubick, Robert J.: Some Effects of Rapid Inlet Pressure Oscillations on the Operation of a Turbojet Engine. NACA RM E58A03, 1958.

4. Langston, C. E.: Distortion Tolerance - By Design Instead of by Accident. Paper 69-GT-115, ASME, Mar. 1969.

5. Bellman, Donald R.; and Hughes, Donald L.: The Flight Investigation of Pressure Phenomena in the Air Intake of an F-111A Airplane. Paper 69-488, AIAA, June 1969.

6. Meyer, Carl L.; McAulay, John E.; and Biesiadny, Thomas J.: Technique for Inducing Controlled Steady-State and Dynamic Inlet Pressure Disturbances for Jet Engine Tests. NASA TM X-1946, 1970.

7. Baumbick, Robert J.: Device for Producing Dynamic Distortion Patterns at Inlets of Air-Breathing Engines. NASA TM X-2026, 1970.

8. Staff of the Lewis Laboratory: Central Automatic Data Processing System. NACA TN 4212, 1958.

9. Braithwaite, Willis M.; Dicus, John H.; and Moss, John E.: Evaluation with a Turbofan Engine of Air Jets as a Steady-State Inlet Flow Distortion Device. NASA TM X-1955, 1970.

10. Wenzel, Leon M.: Experimental Investigation of the Effects of Pulse Pressure Distortions Imposed on the Inlet of a Turbofan Engine. NASA TM X-1928, 1969.

NATIONAL AERONAUTICS AND SPACE ADMINISTRATION
WASHINGTON, D. C. 20546

OFFICIAL BUSINESS

FIRST CLASS MAIL

POSTAGE AND FEES PAID
NATIONAL AERONAUTICS AN
SPACE ADMINISTRATION

POSTMASTER: If Undeliverable (Section 158 Postal Manual) Do Not Return

"The aeronautical and space activities of the United States shall be conducted so as to contribute . . . to the expansion of human knowledge of phenomena in the atmosphere and space. The Administration shall provide for the widest practicable and appropriate dissemination of information concerning its activities and the results thereof."

—NATIONAL AERONAUTICS AND SPACE ACT OF 1958

NASA SCIENTIFIC AND TECHNICAL PUBLICATIONS

TECHNICAL REPORTS: Scientific and technical information considered important, complete, and a lasting contribution to existing knowledge.

TECHNICAL NOTES: Information less broad in scope but nevertheless of importance as a contribution to existing knowledge.

TECHNICAL MEMORANDUMS: Information receiving limited distribution because of preliminary data, security classification, or other reasons.

CONTRACTOR REPORTS: Scientific and technical information generated under a NASA contract or grant and considered an important contribution to existing knowledge.

TECHNICAL TRANSLATIONS: Information published in a foreign language considered to merit NASA distribution in English.

SPECIAL PUBLICATIONS: Information derived from or of value to NASA activities. Publications include conference proceedings, monographs, data compilations, handbooks, sourcebooks, and special bibliographies.

TECHNOLOGY UTILIZATION PUBLICATIONS: Information on technology used by NASA that may be of particular interest in commercial and other non-aerospace applications. Publications include Tech Briefs, Technology Utilization Reports and Notes, and Technology Surveys.

Details on the availability of these publications may be obtained from:

SCIENTIFIC AND TECHNICAL INFORMATION DIVISION

NATIONAL AERONAUTICS AND SPACE ADMINISTRATION

Washington, D.C. 20546